

The Pristine survey – X. A large population of low-metallicity stars permeates the Galactic disc

Federico Sestito,^{1,2*} Nicolas F. Martin,^{1,3} Else Starckenburg,² Anke Arentsen²,
 Rodrigo A. Ibata,¹ Nicolas Longeard,⁴ Collin Kiely⁵,⁵ Kristopher Youakim²,²
 Kim A. Venn⁵,⁵ David S. Aguado,⁶ Raymond G. Carlberg,⁷
 Jonay I. González Hernández,^{8,9} Vanessa Hill,¹⁰ Pascale Jablonka,^{4,11}
 Georges Kordopatis,¹⁰ Khyati Malhan,¹² Julio F. Navarro,⁵ Rubén Sánchez-Janssen,¹³
 Guillame Thomas,¹⁴ Eline Tolstoy,¹⁵ Thomas G. Wilson^{16,17},^{16,17} Pedro A. Palicio,^{8,9,10}
 Spencer Bialek,⁵ Rafael Garcia-Dias⁸,⁸ Romain Lucchesi,⁴ Pierre North,⁴
 Yeisson Osorio⁸,⁸ Lee R. Patrick⁸ and Luis Peralta de Arriba^{6,16}

Affiliations are listed at the end of the paper

Accepted 2020 February 5. Received 2020 February 5; in original form 2019 November 19

ABSTRACT

The orbits of the least chemically enriched stars open a window on the formation of our Galaxy when it was still in its infancy. The common picture is that these low-metallicity stars are distributed as an isotropic, pressure-supported component since these stars were either accreted from the early building blocks of the assembling Milky Way (MW), or were later brought by the accretion of faint dwarf galaxies. Combining the metallicities and radial velocities from the Pristine and LAMOST surveys and *Gaia* DR2 parallaxes and proper motions for an unprecedented large and unbiased sample of 1027 very metal poor stars at $[\text{Fe}/\text{H}] \leq -2.5$ dex, we show that this picture is incomplete. We find that 31 per cent of the stars that currently reside spatially in the disc ($|Z| \leq 3$ kpc) do not venture outside of the disc plane throughout their orbit. Moreover, this sample shows strong statistical evidence (at the 5.0σ level) of asymmetry in their kinematics, favouring prograde motion. The discovery of this population implies that a significant fraction of stars with iron abundances $[\text{Fe}/\text{H}] \leq -2.5$ dex merged into, formed within, or formed concurrently with the MW disc and that the history of the disc was quiet enough to allow them to retain their disc-like orbital properties, challenging theoretical and cosmological models.

Key words: Galaxy: abundances – Galaxy: disc – Galaxy: evolution – Galaxy: formation – Galaxy: halo – Galaxy: kinematics and dynamics.

1 INTRODUCTION

As successive generations of stars are formed from the gaseous material that is chemically enriched by earlier generations of stars, the most chemically pristine stars provide a unique window into the oldest components of the Milky Way (hereafter MW; Freeman & Bland-Hawthorn 2002; Karlsson, Bromm & Bland-Hawthorn 2013), dating back to times when our Galaxy was still assembling. It is expected that low-metallicity stars, whose iron abundance is lower than a few thousands of the Sun's

($[\text{Fe}/\text{H}] \leq -2.5$ dex) were formed at most 2–3 Gyr after the big bang (El-Badry et al. 2018). Since the then proto-Milky Way was still in the process of chaotically accreting, it is commonly expected that the most metal-poor stars mainly trace the spheroid of the MW. These stars should either be present in the deepest parts of the Galactic potential well if they were accreted at the formation of the MW, or further out in the stellar halo if they formed in dwarf galaxies that were accreted on to the MW at later times (White & Springel 2000; Brook et al. 2007; Gao et al. 2010; Salvadori et al. 2010; Tumlinson 2010; Ishiyama et al. 2016; Starckenburg et al. 2017a; El-Badry et al. 2018; Griffen et al. 2018). The inescapable conclusion of this scenario is that low-metallicity stars should follow pressure-supported orbits and that they should be most prominent in

* E-mail: federico.sestito@astro.unistra.fr

the central regions of the MW or in its diffuse stellar halo. Moreover, these stars should be absent from the MW disc because stars formed very early in the proto-disc were scattered into the halo during the dynamic assembly process. The disc's successive generation of stars are expected to have formed from already enriched gas.

Recent work by Sestito et al. (2019) has shown the orbital properties of the 42 most pristine stars known in the ultra metal-poor regime (UMP, $[\text{Fe}/\text{H}] < -4.0$ dex) using the photometric and kinematic data of the Data Release 2 (DR2) of the *Gaia* satellite (Gaia Collaboration 2016, 2018). Surprisingly, roughly a quarter of those stars orbit close or within the plane of the MW disc. Whilst tentative, the small size of the sample and inhomogeneous data collection methods in this literature sample prevent a firm conclusion on the orbital parameters of the most metal-poor stars.¹ In this work, we revisit these interesting findings with our more unbiased and very large sample of stars, putting the work on the orbital properties of very metal-poor stars (VMP) on a much firmer statistical footing.

In general, the rarity of low-metallicity stars among the bulk of the more metal-rich MW stars has long limited the mapping of their distribution. However, recent, systematic, and large spectroscopic surveys (Allende Prieto et al. 2014; Li, Tan & Zhao 2018) and specific photometric surveys (Starkenburg et al. 2017b; Wolf et al. 2018) yield increasingly large spectroscopic samples of such stars. In this work, we use two well-known samples of VMP stars ($[\text{Fe}/\text{H}] \leq -2.0$ dex) in order to study the orbital properties of the most metal-poor stars focussing on the disc region. The Large sky Area Multi-Object fiber Spectroscopic Telescope (LAMOST; Cui et al. 2012) probes all Galactic latitudes and does not select stars to specifically focus on the regions of the MW halo at high Galactic latitudes. We complement this sample with VMPs from the spectroscopic follow-up campaign of the Pristine survey (Youakim et al. 2017; Aguado et al. 2019). The resulting combined sample of 1027 stars below $[\text{Fe}/\text{H}] \leq -2.5$ dex from LAMOST (667 stars) and the Pristine survey (360 stars), with the synergy of the exquisite *Gaia* DR2 data, provides a unique data set to study the orbital properties of VMP stars, as it is both large and selected purely on metallicity without any pre-selection on kinematics.

We describe the data samples in Section 2, before turning to our results in Section 3 and implications for our understanding of the formation and (early) evolution of the MW galaxy in Section 4.

2 DATA

2.1 The Pristine sample

The Pristine survey is a photometric survey that aims at efficiently finding the most metal-poor stars (Starkenburg et al. 2017b). It is based on narrow-band Ca H&K photometry obtained with the MegaCam wide-field camera on the 3.6 m Canada–France–Hawaii Telescope (CFHT). In this work, we use the VMP stars ($[\text{Fe}/\text{H}] < -2.0$ dex) photometrically selected from the narrow-band photometry and then spectroscopically followed-up with the IDS spectrograph at the 2.54 m Isaac Newton Telescope (INT) at Observatorio del Roque de los Muchachos. This sample and its analysis are described in Aguado et al. (2019). The sample is composed of 576 genuine VMP stars, of which 360 with $[\text{Fe}/\text{H}] \leq -2.5$ dex, 66 are EMP stars ($[\text{Fe}/\text{H}] < -3.0$ dex), and none

are UMP. The sample spans a magnitude range of $11.5 \leq G \leq 16.5$ mag. We derive the radial velocities of these VMP stars using the `fxcor` task (a Fourier cross-correlation method) from IRAF (Tody 1986, 1993) with an appropriate synthetic template spectra for each star matching within 250 K in temperature, 0.5 dex in $[\text{Fe}/\text{H}]$, and 1 dex in carbon abundance. A sub-sample of these stars (~ 20) was subsequently followed-up with high-resolution at CFHT with Echelle SpectroPolarimetric Device for the Observation of Stars (ESPaDOnS; Donati 2003; Donati et al. 2006; Venn et al. 2019) and at Gemini with GRACES (Gemini Remote Access to CFHT ESPaDOnS Spectrograph, Chene et al. 2014, Kieley et al. in preparation). From this overlapping sub-sample, we assessed the magnitude of any systematic errors on the radial velocities and found a systematic offset of $\mu_{\text{off}} = 4.9 \pm 3.4 \text{ km s}^{-1}$ in the mean and a standard deviation between both sets of measurements of $\sigma_{\text{sys}} = 10.5 \pm 4.1 \text{ km s}^{-1}$. Together with the individual measurement uncertainties on the radial velocity derivation, these uncertainties are propagated in the derivation of the orbital parameters and their uncertainties.

2.2 The LAMOST sample

Li et al. (2018) presented new metallicities for a set of 10 000 VMP star candidates from LAMOST DR3 (Cui et al. 2012; Zhao et al. 2012), spanning a magnitude range of $9.0 \leq G \leq 18.0$ mag. We note there is a spurious effect in this VMP sample, and ~ 5 per cent of stars accumulate at the lower effective temperature limit of the employed model grid. Our own analysis shows these are spurious metal-rich stars that contaminate the sample. Therefore, we clean this sample accordingly, resulting a final selection of 4838 VMP stars, of which 667 have $[\text{Fe}/\text{H}] \leq -2.5$ dex, 41 are EMP, and none are UMP. For a detailed description of the cleaning steps see Appendix A and Fig. A1–A2 therein (available online).

2.3 Determination of distances and orbital properties

We infer distances for stars from both surveys following the Bayesian method described in Sestito et al. (2019). In short, we derive a probability distribution function (PDF) of the heliocentric distance to a star by combining its photometric (G , BP , and RP magnitudes) and astrometric data (parallax ϖ) from *Gaia* DR2 with a sensible MW stellar density prior and MESA/MIST isochrone models (Choi et al. 2016; Dotter 2016) for stars of old age (> 11 Gyr). This Bayesian method to infer distance does not require a reliable parallax measurement, but does take into account all parallax information available (even negative values). As discussed in Sestito et al. (2019), the choice of the MW density prior affects the results only when the distance PDF has two solutions (i.e. both a dwarf and a giant solution) changing the probabilities associated with the two solutions, but not the values of the distances. After finding that a significant fraction of UMP stars reside close to the MW plane (Sestito et al. 2019), we therefore chose an MW density prior composed by the sum of a halo component described by a power law, and a disc component described by an exponential distribution law. Subsequently, we derive the orbits using the `galpy` code² (Bovy 2015) providing it with the inferred distances, the radial velocities, and the exquisite *Gaia* DR2 proper motions, together with the uncertainties and systematics. For the gravitational

¹Very similar kinematical signatures are found by Di Matteo et al. (2019) for a small sample of 54 stars peaked around $[\text{Fe}/\text{H}] = -3$ dex.

²The PYTHON package for Galactic dynamics Galpy by Bovy (2015) can be found at <http://github.com/jobovy/galpy>.

potential, we use a more massive halo ($1.2 \times 10^{12} M_{\odot}$) compared to *MWPotential14* from GALPY ($0.8 \times 10^{12} M_{\odot}$) in agreement with the value from Bland-Hawthorn & Gerhard (2016), an exponentially cut-off bulge, a Miyamoto Nagai Potential disc, and a Navarro, Frenk & White (1997) dark matter halo. The Local Standard of Rest circular velocity, Sun peculiar motion, and distance from the Galactic Centre are the same as assumed by Sestito et al. (2019; see also references therein). The table with the inferred orbital parameters is provided as online material.

The possible bias towards giants or dwarfs due to observational constraints in the Pristine and LAMOST survey is expected to not produce a bias in the prograde versus retrograde population, and therefore in our main result.

3 RESULTS

We derive the orbital properties of our sample, focussing on the following quantities: the azimuthal action J_{ϕ} , which is equivalent to the z -axis component of a star's angular momentum; the vertical action, J_z , which conveys information about how far a star's orbit brings it away from the Galactic plane; and the eccentricity of the orbit, ϵ . The top panel of Fig. 1 shows the distribution of stars in the J_z - J_{ϕ} plane, colour coded by the eccentricity of a given star's orbit, for our full sample with $[\text{Fe}/\text{H}] \leq -2.5$ dex, complemented by the 42 UMP stars ($[\text{Fe}/\text{H}] \leq -4.0$ dex) from Sestito et al. (2019). We see a clear population of stars that remain close to the MW plane (very small J_z), although not all of these stars are on perfectly circular orbits. More importantly, the sample exhibits a strong asymmetry between prograde ($J_{\phi} > 0$) and retrograde ($J_{\phi} < 0$) stars, where prograde stars dominate with an angular momentum up to the Sun's value.

The bottom panels of Fig. 1 show the same action plot divided into four metallicity bins, respectively the UMP stars populated only by the 42 stars from Sestito et al. (2019), the $-4.0 < [\text{Fe}/\text{H}] \leq -3.0$ dex bin, the $-3.0 < [\text{Fe}/\text{H}] \leq -2.5$ dex regime, and, to be complete, the bin with $-2.5 < [\text{Fe}/\text{H}] \leq -2.0$ dex, where the signature of a disc population is well studied (Beers et al. 2002; Reddy & Lambert 2008; Ruchti et al. 2011; Li & Zhao 2017). We note that Carollo et al. (2019) already report signatures of the disc population to a metallicity of $[\text{Fe}/\text{H}] \gtrsim -3.0$ dex. Separating the sample in these metallicity bins makes it evident that the prograde stars that remain close to the MW plane inhabit all $[\text{Fe}/\text{H}]$ ranges. Focussing on the region of the diagram that is populated by disc-like stars, with $0.5 < J_{\phi}/J_{\phi\odot} < 1.2$ and $J_z/J_{z\odot} < 0.125 \times 10^4$, we assess the significance of the asymmetry through a direct comparison with the retrograde stars of similar properties ($-1.2 < J_{\phi}/J_{\phi\odot} < -0.5$ and same $J_z/J_{z\odot}$ range). Assuming Poisson statistics, we find that the prograde region is 5.0σ overdense compared to its retrograde counterpart for the $[\text{Fe}/\text{H}] \leq -2.5$ dex regime, or 1.9σ overdense for the $[\text{Fe}/\text{H}] < -3.0$ dex. For these two regimes, the overdensity of disc-like stars in the prograde box remains similar and the lower significance in the lower metallicity bin is driven by the smaller numbers. When adopting a two-dimensional Kolmogorov–Smirnov test (Peacock 1983; Fasano & Franceschini 1987) we find that we can discard the hypothesis that these different samples, from the ultra metal-poor regime to the VMP regime (VMP, $[\text{Fe}/\text{H}] < -2.0$ dex), are drawn from a different parent distribution. There is no bias we can think of in the two surveys at the base of our sample that would preferentially overselect prograde over retrograde stars. In particular, no selection on the motion of stars was applied to either of the two surveys that were designed before the *Gaia* DR2

data were available. We have tested that our results are similar whether we restrict ourselves only to these stars with reliable parallax information (see Appendix B and B1 therein, available online).

In order to quantify the underlying fraction of disc-like stars in the low-metallicity regime, we look at the population of low-metallicity stars located within 3 kpc of the MW plane. From this selection, we can identify two samples, (i) the disc-like stars with the maximum excursion from the MW plane $|Z_{\text{max}}| \leq 3$ kpc in a prograde motion ($J_{\phi}/J_{\phi\odot} > 0$) and (ii) the halo-like stars that are either passing through the disc or that are close to the plane in a retrograde motion. Of the population of stars with $[\text{Fe}/\text{H}] \leq -2.5$ dex and with $|Z| < 3$ kpc, ~ 31 per cent belongs to the disc-like sample (i). Although a disc-like component of the MW has been confirmed down to $[\text{Fe}/\text{H}] = -2.3$ dex (e.g. Li & Zhao 2017), and more recently, Carollo et al. (2019) reported a signature to $[\text{Fe}/\text{H}] \gtrsim -3.0$ dex, this is the first time we find strong and statistically significant evidence of such a population for the lowest metallicity stars ($[\text{Fe}/\text{H}] \leq -2.5$ dex). We conclude that an important fraction of the 1069 low-metallicity stars from our sample plus the Sestito et al. (2019) UMP sample in fact reside in the MW disc.

4 DISCUSSION AND CONCLUSION

Understanding the origins of these stars has major implication for the assembly and evolution of the MW. Simulated disc galaxies for which maps are published of low-metallicity stars with $[\text{Fe}/\text{H}] \leq -2.5$ dex in either density (Tumlinson 2010; Starkenburg et al. 2017a) or kinematical space (El-Badry et al. 2018) do not commonly bear this feature. This is either due to the MW having a unique formation path or to these simulations not including all the necessary physical ingredients to produce such a feature. We propose three different scenarios to explain this observational feature: minor mergers, the assembly of the proto-MW, and the *in situ* formation of this component of the disc at early times. We note that these scenarios are not mutually exclusive.

First, it is possible that the observed low-metallicity stars were brought into the MW plane through the minor merging of small satellites that deposited their stars in the environment of the disc, that was already in place, after their orbit decayed via dynamical friction (Scannapieco et al. 2011) and the eccentricity enhanced by tidal interaction (Peñarrubia, Kroupa & Boily 2002; Abadi et al. 2003). Results from cosmological simulations have shown that the disrupted merged satellite can be aligned with the disc (Gómez et al. 2017). Some simulations (Scannapieco et al. 2011; Karademir et al. 2019) show that up to 5–20 per cent of the disc stars have not formed *in situ* but were brought in from now-merged satellites.

Alternatively, or additionally, low-metallicity disc-like stars could have been born in and brought in from the building blocks that formed the disc of the proto-MW at early times. In such a scenario at high redshift, we can expect that whatever gas-rich blocks formed the backbone of the MW disc also brought its own stars, including low-metallicity ones.

Cosmological simulations (El-Badry et al. 2018) show that, of all stars currently within 10 kpc from the MW centre and formed before redshift $z = 5$, less than half were already in the main progenitor at $z = 5$. Over half of these extremely old stars would make their way into the main Galaxy in later merging events and find themselves at $z = 5$ inside different galaxies that are up to 250 kpc away from the main progenitor centre. These two mergers scenarios can naturally funnel stars in the inner regions of the main galaxy, to be observed on orbits close to the disc plane today.

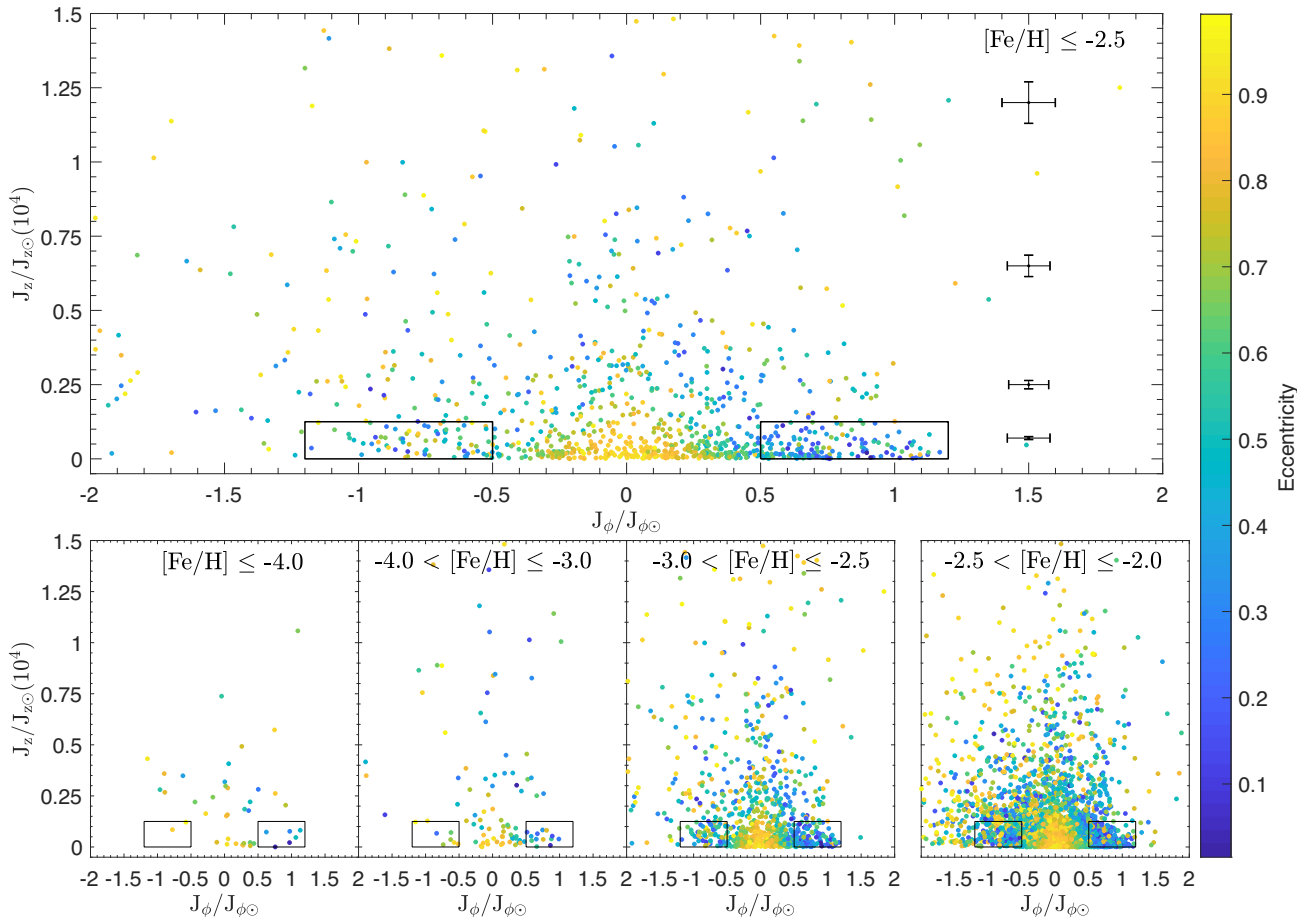


Figure 1. Vertical action versus azimuthal action component colour coded by eccentricity. Top panel: our sample + Sestito et al. (2019) stars with $[\text{Fe}/\text{H}] \leq -2.5$ dex are shown. Typical uncertainties for four bins in $J_z/J_{z\odot}$ are shown on the right. Bottom panels from left to right: our sample + Sestito et al. (2019) stars with $[\text{Fe}/\text{H}] \leq -2.0$ dex is divided into four metallicity ranges. The action quantities are scaled by the solar values (i.e. $J_{\phi\odot} = 2009.92 \text{ km s}^{-1} \text{ kpc}$, $J_{z\odot} = 0.35 \text{ km s}^{-1} \text{ kpc}$). We detect an asymmetry and the predominance for the prograde motion (right box in each panel) versus the retrograde planar stars (left box in each panel) with 5.0σ level for stars with $[\text{Fe}/\text{H}] \leq -2.5$ dex.

For the third scenario, the *in situ* formation at early times, it is necessary to invoke the presence of pockets of pristine gas in the MW’s gaseous disc during the first few Gyr of the Universe. This scenario implies that the MW plane was already defined within 2–3 Gyr and that this plane has not significantly changed over the last 10–11 Gyr. Consequently, the MW cannot have suffered dramatic merger and/or accretion events that would have likely tilted its disc and/or randomized the orbit of the EMP stars (Scannapieco et al. 2009). Such a scenario would be in line with the commonly accepted idea that the MW has undergone a very quiet accretion history (Wyse 2001; Stewart et al. 2008). However, two main questions arise from this scenario. The first question is whether it is possible to form stars so completely devoid of metals in a relatively well-mixed interstellar medium disc in this stage of evolution of the MW. The second question relates to the mechanisms that can push the stars from the small radius of their birth place to the solar neighbourhood and from the likely circular orbit of their birth to the range of observed eccentricities of the orbits we observe them on today. Radial migration is very efficient in pushing outwards the orbital radius whilst conserving their circularity (Sellwood & Binney 2002; Haywood 2008; Schönrich & Binney 2009). For stars with higher orbital eccentricity at birth

(Brook et al. 2004; Bird et al. 2013; Minchev, Chiappini & Martig 2013), radial migration is less efficient (Martig, Minchev & Flynn 2014) but non-linear interactions between the MW bar and its spiral arms (Minchev & Famaey 2010) or perturbations from infalling minor mergers (Quillen et al. 2009) could redistribute their angular momentum.

One important implication of this work is that the disc region should not be avoided in the search and study for the most metal-poor stars, contrary to what has frequently been done in the past. Moreover, cosmological zoom-in simulations should be revisited to reproduce this population of low-metallicity stars with disc-like kinematics. Whatever the true origin of these prominent disc-like low-metallicity stars, they undoubtedly open a window on the assembly of the oldest parts of the MW and pose a challenge to our understanding of very early Galaxy formation in general.

ACKNOWLEDGEMENTS

We want to thank Ivan Minchev for the insightful comments and suggestions on radial migration. We are also grateful to the anonymous referee for their comments and support. This work has made use of data from the European Space Agency (ESA) mission

Gaia (<https://www.cosmos.esa.int/gaia>), processed by the *Gaia* Data Processing and Analysis Consortium (DPAC, <https://www.cosmos.esa.int/web/gaia/dpac/consortium>). Funding for the DPAC has been provided by national institutions, in particular the institutions participating in the *Gaia* Multilateral Agreement. We gratefully acknowledge the Isaac Newton Group (ING) staff, in particular the support astronomers and staff at the INT/WHT for their expertise and help with observations. We also thank the Canada-France-Hawaii Telescope staff for performing the observations in queue mode. Based on observations obtained with MegaPrime/MegaCam, a joint project of CFHT and CEA/DAPNIA, at the Canada-France-Hawaii Telescope (CFHT) which is operated by the National Research Council (NRC) of Canada, the Institut National des Science de l'Univers of the Centre National de la Recherche Scientifique (CNRS) of France, and the University of Hawaii. The observations at the Canada-France-Hawaii Telescope were performed with care and respect from the summit of Maunakea which is a significant cultural and historic site. Guoshoujing Telescope (the Large sky Area Multi-Object fiber Spectroscopic Telescope, LAMOST) is a National Major Scientific Project built by the Chinese Academy of Sciences. FS thanks the Initiative d'Excellence IdEx from the University of Strasbourg and the Programme Doctoral International PDI for funding his Ph.D. This work has been published under the framework of the IdEx Unistra and benefits from a funding from the state managed by the French National Research Agency as part of the investments for the future program. FS, NFM, and RAI gratefully acknowledge support from the French National Research Agency (ANR) funded project 'Pristine' (ANR-18-CE31-0017) along with funding from CNRS/INSU through the Programme National Galaxies et Cosmologie and through the CNRS grant PICS07708. ES, AA, and KY gratefully acknowledge funding by the Emmy Noether program from the Deutsche Forschungsgemeinschaft (DFG). The authors acknowledge the support and funding of the International Space Science Institute (ISSI) for the international team 'Pristine'. FS acknowledges the support and funding of the Erasmus + programme of the European Union.

REFERENCES

- Abadi M. G., Navarro J. F., Steinmetz M., Eke V. R., 2003, *ApJ*, 597, 21
 Aguado D. S. et al., 2019, *MNRAS*, 490, 2241
 Allende Prieto C. et al., 2014, *A&A*, 568, A7
 Beers T. C., Drilling J. S., Rossi S., Chiba M., Rhee J., Führmeister B., Norris J. E., von Hippel T., 2002, *AJ*, 124, 931
 Bird J. C., Kazantzidis S., Weinberg D. H., Guedes J., Callegari S., Mayer L., Madau P., 2013, *ApJ*, 773, 43
 Bland-Hawthorn J., Gerhard O., 2016, *ARA&A*, 54, 529
 Bovy J., 2015, *ApJS*, 216, 29
 Brook C. B., Kawata D., Gibson B. K., Freeman K. C., 2004, *ApJ*, 612, 894
 Brook C. B., Kawata D., Scannapieco E., Martel H., Gibson B. K., 2007, *ApJ*, 661, 10
 Carollo D. et al., 2019, *ApJ*, 887, 22
 Chene A.-N. et al., 2014, in Navarro R., Cunningham C. R., Barto A. A., eds, Proc. SPIE Conf. Ser., Vol. 9151, Advances in Optical and Mechanical Technologies for Telescopes and Instrumentation. SPIE, Bellingham, p. 915147
 Choi J., Dotter A., Conroy C., Cantiello M., Paxton B., Johnson B. D., 2016, *ApJ*, 823, 102
 Cui X.-Q. et al., 2012, *Res. Astron. Astrophys.*, 12, 1197
 Di Matteo P., Spite M., Haywood M., Bonifacio P., Gómez A., Spite F., Caffau E., 2019, preprint ([arXiv:1910.13769](https://arxiv.org/abs/1910.13769))
 Donati J. F., 2003, ASP Conf. Ser. Vol. 307, ESPaDOnS: An Echelle Spectropolarimetric Device for the Observation of Stars at CFHT. Astron. Soc. Pac., San Francisco, p. 41
 Donati J. F., Catala C., Landstreet J. D., Petit P., 2006, ASP Conf. Ser. Vol. 358, ESPaDOnS: The New Generation Stellar Spectro-Polarimeter. Performances and First Results, Astron. Soc. Pac., San Francisco, p. 362
 Dotter A., 2016, *ApJS*, 222, 8
 El-Badry K. et al., 2018, *MNRAS*, 480, 652
 Fasano G., Franceschini A., 1987, *MNRAS*, 225, 155
 Freeman K., Bland-Hawthorn J., 2002, *ARA&A*, 40, 487
 Gaia Collaboration, 2016, *A&A*, 595, A1
 Gaia Collaboration, 2018, *A&A*, 616, A1
 Gao L., Theuns T., Frenk C. S., Jenkins A., Helly J. C., Navarro J., Springel V., White S. D. M., 2010, *MNRAS*, 403, 1283
 Gómez F. A. et al., 2017, *MNRAS*, 472, 3722
 Griffen B. F., Dooley G. A., Ji A. P., O'Shea B. W., Gómez F. A., Frebel A., 2018, *MNRAS*, 474, 443
 Haywood M., 2008, *MNRAS*, 388, 1175
 Ishiyama T., Sudo K., Yokoi S., Hasegawa K., Tominaga N., Susa H., 2016, *ApJ*, 826, 9
 Karademir G. S., Remus R.-S., Burkert A., Dolag K., Hoffmann T. L., Moster B. P., Steinwandel U. P., Zhang J., 2019, *MNRAS*, 487, 318
 Karlsson T., Bromm V., Bland-Hawthorn J., 2013, *Rev. Mod. Phys.*, 85, 809
 Li C., Zhao G., 2017, *ApJ*, 850, 25
 Li H., Tan K., Zhao G., 2018, *ApJS*, 238, 16
 Martig M., Minchev I., Flynn C., 2014, *MNRAS*, 443, 2452
 Minchev I., Famaey B., 2010, *ApJ*, 722, 112
 Minchev I., Chiappini C., Martig M., 2013, *A&A*, 558, A9
 Navarro J. F., Frenk C. S., White S. D. M., 1997, *ApJ*, 490, 493
 Peacock J. A., 1983, *MNRAS*, 202, 615
 Peñarrubia J., Kroupa P., Boily C. M., 2002, *MNRAS*, 333, 779
 Quillen A. C., Minchev I., Bland-Hawthorn J., Haywood M., 2009, *MNRAS*, 397, 1599
 Reddy B. E., Lambert D. L., 2008, *MNRAS*, 391, 95
 Ruchti G. R. et al., 2011, *ApJ*, 737, 9
 Salvadori S., Ferrara A., Schneider R., Scannapieco E., Kawata D., 2010, *MNRAS*, 401, L5
 Scannapieco C., White S. D. M., Springel V., Tissera P. B., 2009, *MNRAS*, 396, 696
 Scannapieco C., White S. D. M., Springel V., Tissera P. B., 2011, *MNRAS*, 417, 154
 Schönrich R., Binney J., 2009, *MNRAS*, 396, 203
 Sellwood J. A., Binney J. J., 2002, *MNRAS*, 336, 785
 Sestito F. et al., 2019, *MNRAS*, 484, 2166
 Starkeburg E., Oman K. A., Navarro J. F., Crain R. A., Fattahi A., Frenk C. S., Sawala T., Schaye J., 2017a, *MNRAS*, 465, 2212
 Starkeburg E. et al., 2017b, *MNRAS*, 471, 2587
 Stewart K. R., Bullock J. S., Wechsler R. H., Maller A. H., Zentner A. R., 2008, *ApJ*, 683, 597
 Tody D., 1986, in Crawford D. L., ed., Proc. SPIE Conf. Ser. Vol. 627, Instrumentation in Astronomy VI. SPIE, Bellingham, p. 733
 Tody D., 1993, in Hanisch R. J., Brissenden R. J. V., Barnes J., eds, ASP Conf. Ser. Vol. 52, Astronomical Data Analysis Software and Systems II. Astron. Soc. Pac., San Francisco, p. 173
 Tumlinson J., 2010, *ApJ*, 708, 1398
 Venn K. et al., 2020, *MNRAS*, 492, 3241
 White S. D. M., Springel V., 2000, in Weiss A., Abel T. G., Hill V., eds, The First Stars. p. 327, Springer-Verlag, Berlin Heidelberg
 Wolf C. et al., 2018, *PASA*, 35, e010
 Wyse R. F. G., 2001, in Funes J. G., Corsini E. M., eds, ASP Conf. Ser. Vol. 230, Galaxy Disks and Disk Galaxies. Astron. Soc. Pac., San Francisco, p. 71
 Youakim K. et al., 2017, *MNRAS*, 472, 2963
 Zhao G., Zhao Y.-H., Chu Y.-Q., Jing Y.-P., Deng L.-C., 2012, *Res. Astron. Astrophys.*, 12, 723

SUPPORTING INFORMATION

Supplementary data are available at [MNRASL](https://www.mnrasl.org) online.

Appendix A. The cleaning of the Lamost sample.

Appendix B. Results with good parallax data.

Please note: Oxford University Press is not responsible for the content or functionality of any supporting materials supplied by the authors. Any queries (other than missing material) should be directed to the corresponding author for the article.

¹*Université de Strasbourg, CNRS, Observatoire astronomique de Strasbourg, UMR 7550, F-67000 Strasbourg, France*

²*Leibniz Institute for Astrophysics Potsdam (AIP), An der Sternwarte 16, D-14482 Potsdam, Germany*

³*Max-Planck-Institut für Astronomie, Königstuhl 17, D-69117 Heidelberg, Germany*

⁴*Institute of Physics, Laboratoire d'astrophysique, École Polytechnique Fédérale de Lausanne (EPFL), Observatoire, CH-1290 Versoix, Switzerland*

⁵*Department of Physics and Astronomy, University of Victoria, PO Box 3055, STN CSC, Victoria, BC V8W 3P6, Canada*

⁶*Institute of Astronomy, University of Cambridge, Madingley Road, Cambridge CB3 0HA, UK*

⁷*Department of Astronomy and Astrophysics, University of Toronto, Toronto, ON M5S 3H4, Canada*

⁸*Instituto de Astrofísica de Canarias, Vía Láctea, E-38205 La Laguna, Tenerife, Spain*

⁹*Departamento de Astrofísica, Universidad de La Laguna, E-38206 La Laguna, Tenerife, Spain*

¹⁰*Laboratoire Lagrange, Université de Nice Sophia-Antipolis, Observatoire de la Côte d'Azur, CNRS, Bd de l'Observatoire, CS 34229, F-06304 Nice cedex 4, France*

¹¹*GEPi, Observatoire de Paris, Université PSL, CNRS, Place Jules Janssen, F-92190 Meudon, France*

¹²*The Oskar Klein Centre for Cosmoparticle Physics, Department of Physics, Stockholm University, AlbaNova, SE-10691 Stockholm, Sweden*

¹³*UK Astronomy Technology Centre, Royal Observatory, Blackford Hill, Edinburgh EH9 3HJ, UK*

¹⁴*NRC Herzberg Astronomy and Astrophysics, 5071 West Saanich Road, Victoria, BC V9E 2E7, Canada*

¹⁵*Kapteyn Astronomical Institute, University of Groningen, Landleven 12, NL-9747AD Groningen, the Netherlands*

¹⁶*Isaac Newton Group of Telescopes, E-38700 Santa Cruz de La Palma, Spain*

¹⁷*SUPA, School of Physics and Astronomy, University of St. Andrews, North Haugh, Fife KY16 9SS, UK*

This paper has been typeset from a $\text{\TeX}/\text{\LaTeX}$ file prepared by the author.